Published in final edited form as:
Neurobiol Dis. 2008 February ; 29(2): 267–277.

Effects of Chronic Network Hyperexcitability on the Growth of Hippocampal Dendrites

Masataka Nishimura[1], **James Owens**[1,2], and **John W. Swann**[1,3]

1*The Cain Foundation Laboratories, Department of Pediatrics, Baylor College of Medicine, Houston TX 77030*

2*Department of Neurology, Baylor College of Medicine, Houston TX 77030*

3*Department of Neuroscience, Baylor College of Medicine, Houston TX 77030*

Abstract

Experiments reported here were motivated by studies in both human epilepsy and animal models in which stunted dendritic arbors are observed. Our goal was to determine if chronic network hyperexcitability alters dendritic growth. Experiments were conducted in hippocampal slice cultures obtained from infant mice that express the fluorescent protein YFP in CA1 hippocampal pyramidal cells. Results showed that 4 days of GABAa receptor blockade produced a 40% decrease in basilar dendritic length. When dendritic growth was followed over this 4 day interval, dendrites in untreated slices doubled in length, however dendrites in bicuculline treated cultures failed to grow. These effects were suppressed by APV - suggesting a dependence on NMDA receptor activation. Activation of the transcription factor CREB was also decreased by chronic network hyperexcitability - pointing to possible molecular events underlying the observed suppression of growth. Taken together, our results suggest that chronic hippocampal network hyperexcitability limits dendritic growth.

Keywords

CREB; Epilepsy; NMDA; Seizure; Slice culture

Introduction

Neuronal activity influences the growth of dendrites during development and such activity-dependent morphological alterations are likely to have important consequences on the ultimate functioning of the central nervous system (Cline, 2001; Wong and Ghosh, 2002;Van and Cline, 2004). Indeed, dendrites appear to be anatomically plastic (Faherty et al., 2003;Chklovskii et al., 2004;Cooke and Woolley, 2005) and their adaptability is especially prominent during development (Rhin and Claiborne, 1990; Dalva et al., 1994; Lendavi et al., 2000;Hua and Smith, 2004). Dendritic abnormalities are also associated with developmental brain disorders (Purpura et al., 1982;Armstrong, 2005;Dierssen and Ramakers, 2006). This is true in epilepsy where a loss of dendritic branches and spines are commonly observed (Ward, 1969;Belichencko et al., 1992;Isokawa et al., 1993;Multani et al., 1994). Both glutamatergic and GABAergic synaptic transmission have been proposed to play important roles in regulating

Address correspondence to: John W. Swann Ph.D., The Cain Foundation Laboratories, 6621 Fannin Street MC 3-6365, Houston TX 77030, Tel: 832-824-3969, Fax: 832-825-4217, Email: jswann@bcm.tmc.edu.

dendritic growth (Barbin et al., 1993;Rajan and Cline, 1998;Sin et al., 2002;Wayman et al., 2006). Although little is known about how neuronal activity regulates the formation of hippocampal circuitry, persistent disruptions in the balance of excitatory -inhibitory networks in hippocampus could result in alterations in dendritic growth which would be expected to impact synaptic connectivity and ultimately network operations.

Previous studies in animal models have reported that brief but recurrent seizures in early-life result in a loss of dendritic spines and branches (Jiang et al., 1998;Swann et al., 2000b). Recurrent seizures have also been reported to produce a reduction in the expression of glutamatergic synaptic protein and postsynaptic scaffolding proteins (Swann et al., 2007b). We have observed similar alterations in synaptic proteins in response to prolonged periods of network hyperexcitability in developing hippocampal slice cultures (Swann et al., 2007a). Building on these observations, we report here that chronic network hyperexcitability in hippocampal cultures reduces the length and branching complexity of CA1 pyramidal cell dendrites. We also show for the first time, that epileptiform activity prevents normal dendrite growth and that this is an NMDA dependent process. Moreover, a number of laboratories have recently examined the molecular mechanisms that underlie activity-dependent growth of dendrites (Redmond et al., 2002;Vaillant et al., 2002;Yu and Malenka, 2003;Van and Cline, 2004;Wayman et al., 2006). Numerous signaling cascades have been implicated in these processes. One consistent finding is that activation of the transcription factor CREB appears to play a central role in mediating activity-dependent dendritic growth (Wong and Ghosh, 2002;Konur and Ghosh, 2005). Our results also show that CREB activation is reduced in neurons that have experienced prolonged periods of neuronal hyperexcitability - implicating alterations in an upstream signaling cascade as a possible contributor to the dendritic abnormalities observed.

Materials and methods

Animals

Thy1YFP-H transgenic mice (Feng et al., 2000) were used in all experiments. The day of birth was designated as postnatal day 0 (P0) and transverse hippocampal slice cultures were prepared on P5 or P6. Maintenance of animals and surgical procedures were approved by the Baylor College of Medicine institutional animal care committee and were in keeping with guidelines established by the National Institutes of Health.

Hippocampal slice cultures

Slice cultures of hippocampus were made as previously described (Stoppini et al., 1991; Al-Noori and Swann, 2000; Swann et al. 2007a). Each hippocampus was **transversely** sliced (375μm thick) **along its dorsal-ventral extent** and transferred to 30mm membrane inserts (Millipore, Bedford, MA). Usually, 4 slices were cultured on one membrane. They were cultured in 1ml Neurobasal A medium supplemented with B-27 (Invitrogen, Carlsbad, CA) and 0.5 mM glutamine (Invitrogen) for 3 days. At that time, 100μM bicuculline (Sigma, St. Louis, MO) was added to the culture medium for an additional 4 days. After a total of 7 days in vitro a variety of studies were undertaken to determine the anatomical and molecular consequences of 4 days of chronic disinhibition. Control sister cultures were handled identically with the exception that they were not treated with bicuculline. In some experiments, slice cultures were co-treated with bicuculline and 50 μM 2-amino-5-phosphonovalerate (APV; Tocris Cookson, St. Louis, MO). In other experiments, the culture medium, which normally contains 5.2 mM potassium, was modified by addition of KCl to produce a final concentration of 12 mM potassium.

Electrophysiological recordings

After 3 DIV or 7 DIV, slice cultures were transferred from the incubator to a custom-built perfusion chamber on the fixed stage of an Axioskop microscope (Zeiss, Thornwood, NY). Slices were submerged throughout the recording session and were continuously perfused at 1.5 to 2 ml/min (regulated by a peristaltic pump)with room temperature (25 ± 2°C), oxygenated ($95\%O_2/5\%CO_2$) ACSF containing (in mM): 1.5 $CaCl_2$, 3.5 KCl, 1.5 $MgSO_4$, 122.75 NaCl, 10 Glucose, 1.25 NaH_2PO_4, 26 $NaHCO_3$ and 10 μM Glycine. At the 7 DIV time point, slices were held in place during perfusion by their adherence to the Millicell membrane. At the 3 DIV time point, attachment to the membrane was not as well formed and therefore a custom built "harp" was place over the slices (constructed of a U-shaped flattened piece of silver wire with thin nylon filaments stretched across it). Stratum pyramidale of CA1 and CA3 was identified and extracellular field potential recordings were obtained from these regions using borosilicate glass electrodes (WPI, Sarasota, FL) electrodes of 4 to 6 MΩ resistance (1.5-2.5μm tip diameter) filled with ACSF in order to avoid possible junction potential artifacts. Extracellular field recordings from CA1 and CA3 were performed sequentially and not simultaneously. Recordings were made using an Axopatch 200A amplifier (Molecular Devices, Sunnyvale, CA), low-pass filtered at 5kHz and digitized at 10-20kHz sampling rates using a Digidata 1322A (Molecular Devices). Data were collected and analyzed using pClamp v.9 (Molecular Devices). Baseline extracellular field recordings were obtained in control ACSF for at least 10 minutes before the perfusate was switched to ACSF containing 50 μM bicuculline (Sigma). In separate experiments, extracellular K^+ was increased to 12mM to induce network hyperexcitability. In both *in vitro* epilepsy models, spontaneous extracellular fields were then **sequentially** recorded from both the CA1 and CA3 subfields of each slice on the membrane to assess the occurrence of synchronized population activity which had features of epileptiform discharges.

Neuronal Tracing and Analysis

After 7 days in culture, slices were fixed overnight in a 4% paraformaldehyde/4% sucrose buffered saline kept at 4°C, washed with 1x PBS and mounted on slides. CA1 neurons with strong YFP fluorescence throughout their dendritic tree and well isolated from other YFP neurons were randomly selected and imaged with a confocal microscope. Basilar dendritic arbors were reconstructed digitally from the image stacks using Neurolucida software (MicroBrightField, Colchester, VT). It was not possible to reconstruct CA1 apical dendrites due to the large number of fluorescent processes in the apical dendritic layer. When following an apical dendrite from the cell body it would repeatedly cross dendrites and axons from other fluorescent CA1 pyramidal cells making it impossible to identify the processes arising from the cell under study. Confocal imaging was accomplished using a FluoView FV300 confocal laser scanning Microscope on a BX50WI fixed stage upright microscope equipped with a FV5-ZM stepper motor and FluoView software (Olympus, Melville, NY). YFP images were acquired via excitation with an argon laser (488 nm line), a 505-525 nm bandpass emission filter set, and a 20× UPlanApo **objective (numerical aperture (NA) = 0.8**, Olympus) using the appropriate manufacturer-suggested confocal apertures. **Steps in the Z-axis were in 2 μm increments**. Kalman accumulation averaging of 3 or 4 was used. Maximum projection images were generated with FluoView software. All Neurolucida reconstructions were conducted in a blinded manner. Quantitative analysis on the traced data was done using Neuroexplorer software (MicroBrightField). Numerical data (total dendritic length and branch points), such as geometric means and SEMs were then calculated for each treatment group and for the control group. Each type of experiment was repeated on three separate occasions and results combined for final analysis. Similar combined confocal imaging and neuron reconstructions have been performed in the past to quantify experimentally-induced alterations in dendrite arbors (Redmond et al., 2002; Jin et al., 2003) and is advantageous over more

traditional biocytin reconstructions which require time-consuming whole cell recordings to fill individual cells.

Immunohistochemistry

Following fixation with 4% paraformaldehyde/4% sucrose, all slices were carefully lifted from the Millipore membranes, placed into individual vials, and rinsed free-floating in 1x PBS. For the following protocol, all immunohistochemical reactions in experimental and control slice cultures were done simultaneously under identical conditions. First slices were rinsed twice in PBS and then once in PBS with 0.3% Triton X-100 (Sigma) at 1hr intervals. The explants were then incubated in a solution containing the primary antibody for 3 days at 4°C. This solution consisted of 1x PBS, 0.3% Triton X-100 and the primary rabbit antibody, anti-phospho-CREB or anti-CREB (1:1000, Upstate, Lake Placid, NY). After rinsing the explants three times in PBS, the tissue was then incubated for 2 h with Cy5- conjugated goat anti-rabbit secondary antibody (1:1000, Jackson Immunoresearch, West Grove, PA) dissolved in PBS containing 0.3% Triton X-100. The tissue was again rinsed three times in PBS and all sections were then mounted on slides with Vectashield mounting media (Vector Laboratories, Burlingame, CA) and glass coverslips. Images of Cy5 labeled neurons were obtained using a Krypton laser (568 nm line) of a FluoView FV300 microscope and a long pass emission filter BA660IF. YFP images were obtained as described above and overlaid (merged) images were produced by sequential excitation of YFP and Cy5. To quantify bicuculline-induced alterations in Cy5 signal in slice cultures confocal images, collected with a PlanApo 60x objective **(NA = 1.40)**, were imported as 8-bit TIFF files and processed in Adobe Photoshop (Adobe Systems Inc., San Jose, CA). To measure differences in intensity of immunohistochemical staining of nuclei, all nuclei in a chosen image were selected for analysis and the average pixel intensity (level of luminosity) for the nuclei was computed by the software. To correct for variations in background staining from slice to slice, the average pixel intensity of the non-nuclear areas in an image were subtracted from the intensity of nuclear areas in that same image. 8 slice cultures (4 control and 4 bicuculline treated) were analyzed in this manner and three images (at 10 μm steps in the Z axis) were analyzed from each slice.

Statistics

ORIGIN Version 7.5 (OriginLab, Northampton, MA) was employed for construction of histograms and graphs. The data were analyzed statistically using a one-way ANOVA or a two-way ANOVA and a Tukey *post hoc* test to correct for multiple comparisons (Sigma Stat Version 3.5: Systat Software Inc., San Jose, CA). Cumulative probability plots (Figure 2C) were analyzed using a Kolmogorov-Smirnov test (Clampfit Version 9.2: Molecular Devices). In those instances (Figure 2 and 5) when data were not normally distributed, a Kruskal-Wallis one-way ANOVA on Ranks test was applied. A Dunn's Method *post hoc* test to correct for multiple pairwise comparisons confirmed statistical significance (reported as $p < 0.05$). All data were presented as the mean ± SEM.

Results

Bicuculline induces epileptiform activity in slice cultures

In order to establish that neonatal mouse slice cultures treated with bicuculline develop spontaneous synchronized network activity we assessed the effect of acute bicuculline treatment on slice cultures grown in normal media. **Slice cultures were made on P5 or 6** and following either 3 or 7 DIV, slice cultures were transferred to a recording chamber and perfused with normal ACSF followed by ACSF containing 50 μM bicuculline. Figure 1 shows representative extracellular field recordings. Under control conditions (normal ACSF) no spontaneous synchronized activity was observed on 3 DIV, but addition of bicuculline resulted in recurrent spontaneous epileptiform discharges in both area CA1 and CA3 in all slices

examined (9 out of 9 slices). The mean burst duration and the inter-burst interval were nearly identical in the two areas (CA1:duration 0.72 ± 0.25 seconds; inter-burst interval 50.79 ± 50.66 seconds; CA3: duration 0.69 ± 0.16 seconds; inter-burst interval 49.72 ± 40.68 seconds). These results are in keeping with previous recordings from acute brain slices, where recurrent excitatory collaterals between CA3 pyramidal cells are thought to initiate discharging which then spreads to area CA1 through the Schaffer collateral pathway. At the 7 DIV time point, perfusion with bicuculline also resulted in robust recurrent spontaneous epileptiform discharges in both area CA1 and CA3 in each of 15 slices examined (data not shown). Again, mean burst duration and inter-burst interval did not differ significantly between CA1 (duration 1.20 ± 0.69 seconds; inter-burst interval 26.30 ± 14.82 seconds) and CA3 (duration 0.96 ± 0.25 seconds; inter-burst interval 20.35 ± 8.73 seconds). Discharges recorded at the 7 DIV timepoint were longer and more frequent than those recorded at the 3 DIV timepoint (ANOVA - duration: $F(1,44) = 10.03$, $p \leq 0.01$, ANOVA - inter-burst interval: $F(1,44) = 8.02$, $p \leq 0.01$). We have routinely recorded for over 1 hour after network discharging was initiated. Over this time, the characteristics of these events (frequency, duration and amplitude) remained quite stable.

The length and branching complexity of dendritic arbors are reduced by chronic disinhibition

To determine if chronic disinhibition alters dendritic morphology, slices were treated from 3 DIV until 7 DIV with bicuculline. Individual CA1 pyramidal cells were then confocally imaged and basilar dendritic arbors reconstructed using Neurolucida. It was not possible to analyze apical dendrites since they crossed and overlapped with many other processes present in the apical dendritic layer. Figure 2 summarizes results from 3 separate experiments in which the dendrites from 18 control and 17 bicuculline-treated neurons were reconstructed. The bar graphs in Figure 2A show that following 4 days of chronic disinhibition a 40.6% decrease in dendritic length was observed (Control: 1736 ± 135.5 versus Bicuculline: 1031 ± 72.2 μm, $p \leq 0.001$). In Figure 2B, the number of branch points in basilar dendritic arbors is shown to also be significantly decreased by 33.6% (Control: 17.4 ± 1.4 versus Bicuculline: 11.6 ± 1.6, $p \leq 0.01$). This latter result led us to suspect that the reduction in dendritic length shown in Figure 2A may be solely the product of a decrease in the number of dendritic branches. However, this did not appear to be the case. In Figure 2C, the cumulative probability plot indicates that a higher percentage of dendritic segments are uniformly shorter after bicuculline treatment **($p \leq 0.01$, Kolmogorov-Smirnov test)**. The bar graph in the inset shows that the average length of individual segments is significantly smaller (Control: 43.0 ± 1.7 versus Bicuculline: 36.7 ± 1.7μm, $p \leq 0.05$). Terminal order segments of dendrites are thought to be sites where the majority of dendritic growth takes place (Rajan and Cline, 1998). Based on this, we also examined alterations in the length of terminal order dendritic segments alone. Bicuculline treatment significantly decreased the length of terminal segments by 21% (Control: 52.2 ± 2.5 versus Bicuculline: 41.1 ± 2.4μm, $p \leq 0.001$) - again suggesting that chronic disinhibition not only reduces the addition of new branches but also the growth of existing dendritic segments. Figure 3 shows maximum projection confocal images of representative neurons from the control (Figure 3A) and bicuculline (Figure 3B) treated groups. Figures 3C and D show Neurolucida reconstructions of the cell bodies and basilar dendrites of the cells in A and B and clearly illustrates that neurons treated with bicuculline have shorter dendritic arbors with fewer branches.

At this point it seemed possible that the alterations in dendrite arbors induced by disinhibition might not result from network hyperexcitability but instead could be due to direct effects of GABAa receptor blockade. To address this possibility, we attempted to reproduce the results in Figure 2 by raising extracellular K^+ to 12 mM to increase neuronal and network excitability. To establish that 12mM K^+ was indeed able to induce synchronized network discharging in our slice cultures, extracellular field recordings were made while switching the chamber perfusate from ACSF containing 5.2mM K^+ to 12 mM K^+. In 5.2mM K^+, synchronized

discharging was not recorded. However, upon switching to 12mM K^+ all slice cultures tested (DIV 3: 7 slices, DIV 7: 12 slices) displayed frequent (interevent intervals 0.32 to 2.5 sec) recurrent synchronized population discharges.

Based on these results, we examined the effects of a 4 day (DIV 3-7) high K^+ treatment on dendrites. Results showed that as with bicuculline treatment the length of YFP-positive basilar dendrites was decreased (49%) by this alternative treatment (Control: 1188 ± 175.0 versus KCl: 606.7 ± 62.3 μm, $p \leq 0.05$; n =8 and 7 respectively). In addition, the average length of individual segments was significantly smaller (Control: 43.3 ± 2.5 versus KCl: 27.8 ± 1.8μm, $p \leq 0.001$), as was the length of terminal segments (Control: 57.6 ± 3.4 versus KCl: 33.3 ± 2.6μm, $p \leq 0.001$). The number of dendritic branch points was also reduced 24.6% (Control: 11.8 ± 1.6 versus KCl: 8.9 ± 1.3μm). Since the effects of high K^+ reproduced those of bicuculline, we concluded that the effects of bicuculline were mediated primarily by enhanced neuronal excitability.

Chronic disinhibition blocks the growth of dendrites

There are a number of ways in which chronic bicuculline treatment could reduce the length and branching complexity of dendritic arbors. One possibility is that network hyperexcitability damages the dendrites of developing pyramidal cells and reduces branching complexity by eliminating damaged segments or portions of segments. Typically, when dendrites are damaged by excitotoxic injury they display varicose swellings (Swann et al., 2000a). However, in the studies we have conducted thus far we have never observed such swellings in bicuculline-treated slice cultures. In keeping with these observations are other results from this *in vitro* model in which neuronal cell death was not observed (Swann et al., 2007a). Besides excitotoxic injury, another possible explanation for the observed stunted dendrites was that chronic disinhibition retarded the growth of dendrites. To address this possibility slice cultures were fixed at different times after initiation of bicuculline treatment. Control slices served to monitor the normal growth of dendrites in slice cultures. Results in Figure 4A show, that between 3 DIV and 7 DIV, the average length of the basilar dendrites doubled (1016.1 ± 80.1 versus 2128.7 ± 117.8 μm, $p \leq 0.001$). However, at the same time basilar dendrites in bicuculline treated cultures failed to increase and actually decreased slightly in total length (1016.1 ± 80.1 versus 884.8 ± 109.1 μm, $p = 0.767$). Indeed a two way ANOVA revealed that the effects of bicuculline treatment was significantly different from controls ($F(1,76) = 67.7$, $p \leq 0.001$) as was the effects of time in culture ($F(3,76) = 9.03$, $p \leq 0.001$). At 4, 5 and 7 DIV, the length of dendrites in bicuculline treated slices differed significantly from their control counterparts ($p \leq 0.05$).

Figure 4B shows concomitant alterations in basilar dendritic branch points. The number of branch points gradually increased in control slices between 3 and 7 DIV (3DIV: 12.1 ± 1.2 versus 7DIV: 19.2 ± 1.8, $p \leq 0.01$). However, the number of branch points failed to increase and appeared to decrease during bicuculline treatment, but this seeming time-dependent reduction was not statistically significant (3DIV: 12.1 ± 1.2 versus 7DIV: 10.4 ± 1.6, $p > 0.05$, versus 4DIV: 9.2 ± 1.2, $p > 0.05$). However, at 4, 5 and 7 DIV, the number of dendritic branches in bicuculline treated slices differed from those of control slices ($p \leq 0.05$). Again the effects of bicuculline treatment on the total length of dendrites could not be explained solely by the decrease in the number of dendritic branches since when the mean length of dendritic segments were compared in Figure 4C a difference in average segment length was observed at 7 DIV (7DIV Control: 48.9 ± 2.1 versus 7DIV Bicuculline: 36.7 ± 2.6 μm, $p \leq 0.001$). However, unlike the effects on branch points this effect took several days to become apparent. The dendrite reconstructions shown in Figure 4D illustrate results summarized in Figure 4A-C. Between 3 and 7 DIV dendrites from pyramidal cells in control slices show a gradual but

dramatic increase in overall length and branching complexity. These developmental changes are completely absent in bicuculline treated slice cultures.

A role for NMDA receptors in disinhibition-induced alteration in dendrites

Previous studies have implicated activation of NMDA receptors as an important contributor to activity-dependent dendritic growth (Rajan and Cline, 1998;Wayman et al., 2006). Thus we were motivated to determine if a persistent over-activation of NMDA receptors during network hyperexcitability plays a role in the cessation of growth observed in Figure 4. The results of 3 such experiments are shown in Figures 5. As before in these experiments, slice cultures were treated from day 3 *in vitro* with bicuculline. A separate group was co-treated with bicuculline and 50μM d-APV. Controls consisted of untreated slices and a group treated with only APV. Slices were fixed on 7DIV. Results in Figure 5A show that as before bicuculline resulted in a decrease in the total length of basilar dendrites (Control: 1122.2 ± 112.3 versus Bicuculline: 656.3 ± 44.6 μm, $p \leq 0.001$). But when slices were co-treated with bicuculline and APV the total length of the dendritic arbors was not statistically different from the control group (Control: 1122.2 ± 112.3 versus APV + Bicuculline: 1023.1 ± 75.1 μm, $p > 0.05$) but was significantly larger than the bicuculline treated group (APV + Bicuculline: 1023.1 ± 75.1 versus Bicuculline: 656.3 ± 44.6 μm, $p \leq 0.0\,01$). This suggests that at least in terms of total dendritic length APV blocked the effects of bicuculline. A similar result was observed when dendritic branch points were examined (Figure 5B). Again, chronic bicuculline treatment resulted in a decrease in basilar dendritic branch points (Control: 13.6 ± 1.3 versus Bicuculline: 9.1 ± 0.7 μm, $p \leq 0.0\,1$). Dendritic branch number of pyramidal cells in slice cultures that were co-treated with bicuculline and APV were not statistically different from that of the control group (Control: 13.6 ± 1.3 versus APV + Bicuculline: 12.5 ± 1.2, $p > 0.05$) but did differ significantly from cultures treated with bicuculline alone ($p \leq 0.01$). This suggests that APV prevented the decrease in branch number that occurs during bicuculline treatment. APV alone appeared to increase the number of branch points but this also was not statistically significant (Control: 13.6 ± 1.3 versus APV: 17.4 ± 1.2 μm, $p > 0.05$). Since APV rescued total dendritic length when applied with bicuculline, and had effects on branch number we next examined the effects of co-treatment on dendritic segment length. Figure 5C shows that APV abolished the effects of bicuculline on dendritic segment length. This suggests the suppression of dendrite segment growth that is observed in bicuculline treated slices (Control: 35.3 ± 1.4 versus Bicuculline: 29.6 ± 1.4 μm, $p \leq 0.0\,1$) is a NMDA receptor dependent process.

The dendritic reconstruction in Figure 5D supports the results shown in the bar graphs in Figures 5A-C. In these computerized tracings, bicuculline clearly diminishes the length and complexity of basilar dendrites and this effect appears to be abolished by APV. APV alone may increase dendritic arbor complexity in some cells and this could be reflected in the increased number of branch points shown in Figure 5B. However, as mentioned above, this effect was not statistically significant.

Signaling to CREB is altered

Calcium-dependent activation of the transcription factor CREB is thought to play a important role in activity-dependent growth of dendrites (Wong and Ghosh, 2002). A number of signaling cascades including the CAM Kinase and MAP Kinase cascades appear to converge on CREB to mediate their effects (Redmond et al., 2002;Vaillant et al., 2002;Wayman et al., 2006). Since our results suggest that dendritic growth is greatly diminshed by chronic disinhibition we next examined the effects of this treatment on activation of CREB by examining alterations in the phosphorylation at Ser-133. Immunohistochemistry was used to visualize pCREB in hippocampal slice cultures from YFP-H mice, since this allowed us to unequivocally examine pCREB expression in CA1 pyramidal cells. Results are shown in Figure 6 and were obtained on DIV 7, 4 days after initiating bicuculline treatment. In all slices that were treated with

bicuculline a dramatic decrease in the expression of pCREB was observed (Figures 6B and C). Alterations in expression were not restricted to area CA1 since similar decreases in expression were observed in area CA3 and the dentate gyrus (data not shown). At higher magnification (Figures 6D-I), the nuclear localization of pCREB is evident in control slices - especially when merged with images of YFP. Most CA1 pyramidal cells do not express YFP in cultures from YFP-H mice. This contributes to the large number of pCREB and CREB positive cells that are YFP negative in these images (panels B, C, F and I).

Following chronic disinhibition, the level of pCREB expression is quite low (Figure 6H), compared to controls (Figure 6E). When the level of pCREB expression was quantified from images taken from 4 slices, we observed a 42% decrease in expression in area CA1 (Control: 89.0 ± 6.4 versus Bicuculline: 51.7 ± 2.6, $F(1,6) = 29.4$, $p \leq 0.01$). Alterations in pCREB might be explained by a decrease in the expression of the CREB itself. However, this does not appear to be the case. When CREB expression was examined immunohistochemically no difference in expression were observed (Figures 7B and C). CREB was localized to nuclei but the level of expression was very similar in control and bicuculline treated slice cultures (Figures 7E and H). This was confirmed quantitatively since CREB expression showed no difference between the two condition (Control: 92.1 ± 6.7 versus Bicuculline: 87.9 ± 22.4, $F(1,6) = 0.344$, $p = 0.58$). These results suggest that activation of CREB by phosphorylation at Ser133 is reduced by chronic disinhibition.

Discussion

The results reported here show that when hippocampal slice cultures are treated over a 4 day period with a GABAa receptor antagonist, a decrease in basilar dendritic length is observed. This effect is the result of a decrease in both branching complexity and dendritic segment length. These effects appear to result from a complete or near complete suppression of dendritic growth. Between 3 DIV and 7 DIV the dendrites of CA1 pyramidal cells double in length by gradually increasing segment length and branching complexity, however during bicuculline treatment CA1 pyramidal cells seem to stop their elaboration of dendrites and there is no net increase in either segment length or the number of branch points. These effects of bicuculline appear to depend on NMDA receptor function since they were suppressed by the receptor antagonist, APV. Activation of the transcription factor CREB has been implicated in dendrite growth by a number of laboratories. Since in our studies, the expression of pCREB was found to be decreased by chronic disinhibition, alterations in a signaling cascade(s) upstream of CREB could be an important contributor to the suppression of dendritic growth reported here.

Neuronal activity and dendrite growth

The growth of dendrites is a highly dynamic process - consisting of seemingly “trial and error” extensions and retractions of nascent branches (Dailey and Smith, 1996;Wu et al., 1999). Cell-intrinsic molecular programs are known to regulate aspects of dendrite development (Jan and Jan, 2003). However, during postnatal development neuronal activity has also been shown to have a role in dendrite growth. For instance, Sin et al. (Sin et al., 2002) showed in tectal neurons of *Xenopus* that short periods (4 hrs) of enhanced visual activity more than doubled the growth rate of dendrites compared to rates observed in a darkened chamber. Similarly, rats raised in an enriched environment have been reported to have more extensive dendritic arbors (Faherty et al., 2003). Pharmacological blockade of synaptic activity has also been reported to alter dendritic growth (McAllister et al., 1996;Rajan and Cline, 1998;Luthi et al., 2001;Redmond et al., 2002).

However, the results of some of these studies appear paradoxical when compared to results showing neuronal activity promotes growth. For instance, prolonged blockade of glutamate receptors during cortical and hippocampal development with either APV or CNQX has been

reported not to decrease but instead to increase dendritic length and branching complexity (McAllister et al., 1996;Luthi et al., 2001). Furthermore, persistent neuronal hyperexcitability has been reported to decrease dendritic spine density and filopodial dynamic which may be a reflection of diminished dendritic growth (Zha et al., 2005).

Along these same lines, intractable human epilepsy, which is characterized by persistent neuronal hyperexcitability, commonly shows marked decreases in dendritic branching of neocortical and hippocampal neurons (Ward, 1969;Belichencko et al., 1992;Multani et al., 1994). Stunted dendrites have also been observed in numerous animal models of epilepsy (Westrum et al., 1964;Isokawa et al., 1991;Swann et al., 2000b). In accordance with this are more recent reports of decreases in expression of postsynaptic biochemical markers in animal models of early-onset epilepsy, which can not be explained by neuronal cell loss (Swann et al., 2007b).

A likely explanation for seemingly contradictory experimental outcomes - where on the one hand increased activity can promote dendrite growth and on the other prevent it - is the magnitude and duration of changes in neuronal activity that are experimentally induced. When activity is increased within normal physiological ranges and/or over relatively short periods of time (minutes to hours), it can enhance dendrite growth. But when activity is abnormally high for prolonged periods, compensatory mechanisms may be induced that attempt to re-establish normal levels of neuronal activity. In recent years, the cellular and molecular mechanisms responsible for such compensatory or homeostatic mechanisms have been examined (Turrigiano and Nelson, 2004). Numerous effects have been described and the most widely studied have been alterations in glutamatergic synaptic transmission. Experiments have consistently shown that increased neuronal activity, produced by chronic disinhibition, results in diminished glutamatergic synaptic transmission (Turrigiano et al., 1998;O'Brien et al., 1998;Watt et al., 2000). However, with few exceptions (Desai et al., 2002;Burrone et al., 2002;Wierenga et al., 2006) these studies were not explicitly designed to determine the impact of persistent hyperexcitability on neuronal growth and maturation.

Suppression of dendrite growth: Roles for NMDA receptors and CREB signaling

The effects of chronic disinhibition on dendritic growth reported here could be produced in a number of ways. Therefore, it was important to demonstrate that these effects were mediated by neuronal activity. Since NMDA receptors can mediate dendritic growth (Rajan and Cline, 1998;Wayman et al., 2006), we wondered if the suppression of growth we have observed was a NMDA-receptor dependent process - possibly a compensatory response resulting from a persistent over-activation of these glutamate receptors, Results in Figures 5 show that the bicuculline-induced decreases in dendritic length and branching complexity are indeed suppressed by co-treatment with APV. A previous study suggested that the depolarizing actions of GABA in neonatal hippocampus can also mediate dendrite growth (Barbin et al., 1993). Thus a possible explanation for the effects of chronic disinhibition reported here would be that the effects are directly mediated by bicuculline blockade of depolarizing GABA synaptic potentials and not by neuronal network hyperexcitability. However, our most recent studies have shown a dramatic upregulation in the K^+-Cl^- co-transporter, KCC2 in slice cultures during the first 3 days in vitro, which would be expected to produce a hyperpolarizing Cl^- gradient (Swann et al., 2007a). This observation is fully consistent with bicuculline's ability to induce epileptiform activity in slice cultures as early as 3 DIV (Figure 1). Moreover increasing extracellular K^+ reproduced the effects of bicuculline on dendrite length. Taken together, these results coupled with the observation that APV suppresses the effects of bicuculline on dendrite anatomy strongly suggest that the effects are activity and NMDA receptor dependent and not mediated by bicuculline blockade of depolarizing GABA postsynaptic potentials.

These results are also fully consistent with results of biochemical studies of this *in vitro* model (Swann et al., 2007a). Chronic bicuculline treatment has been reported to decrease the expression of numerous dendritic proteins and these effects were blocked by co-treatment with APV. Interestingly, in that study APV was found not to suppress epileptiform discharging. Thus the effects of APV on dendrite growth reported here are likely not due to blockade of synchronized network activity but instead blockade of NMDA receptors activated during epileptiform activity and NMDA receptor-coupled intracellular signaling cascades.

Another study has reported that chronic treatment with APV results in enhanced growth of hippocampal pyramidal cell dendrites in slice cultures (Luthi et al., 2001). While our results showed that APV alone induced a slight increase in total dendritic length and branch points these effects were not significantly different from that of measures of pyramidal cells in control sister cultures. The difference in outcomes from the 2 studies is likely due to different lengths of treatment with APV. In our studies, slices were treated for 4 days but those of Luthi et al. (2001) were for 14 days. It is entirely possible that if we had treated slices for longer periods of time we would have observed increases in dendritic branching, however such experiments were not performed.

Alterations in intracellular Ca^{2+} are well known to influence neuronal differentiation (Spitzer, 2002). Calcium entry through NMDA receptors and voltage gated channels Ca^{2+} channels or release from intracellular stores have all been implicated in aspects of dendritic growth (Redmond et al., 2002;Lohmann et al., 2002;Wayman et al., 2006). Moreover, increases in intracellular Ca^{2+} have been shown to activate transcriptional programs that can mediate dendritic growth. The transcription factor CREB is among the best characterized in this regard (Konur and Ghosh, 2005). Activation of NMDA receptors has been shown to result in activation of CREB by phosphorylation at Ser 133 (Hardingham et al., 2002;Wayman et al., 2006). Numerous upstream signaling cascades can impinge on CREB to influence gene expression and dendrite growth (Wu and Cline, 1998;Wu et al., 2001;Redmond et al., 2002;Vaillant et al., 2002;Wayman et al., 2006). Our studies suggest that following chronic bicuculline treatment the level of pCREB in hippocampal neurons is decreased while the levels of CREB itself remain unaltered. This suggests alterations in an important signaling cascade upstream from CREB could suppress dendritic growth.

Potential clinical implications

Persistent neuronal hyperexcitability accompanies many forms of childhood epilepsy. Children with intractable epilepsy are often cognitively impaired (Hermann et al., 2002; Camfield and Camfield, 2002). It has been debated whether the seizures and accompany neuronal network hyperexcitability contribute to learning disabilities, since a neuropathology could be responsible for both seizures and cognitive impairments. However, recent studies in normal rodents have shown that experimentally-induced recurrent seizures can lead to spatial learning and memory deficits (Holmes et al., 1998;Huang et al., 1999;Lee et al., 2001; Chang et al., 2003). Reduced dendritic arbors following recurrent seizures would be one potential mechanism underlying such learning deficits given that dendrites are the major site of excitatory synaptic transmission and the plasticity thought to underlie formation of memories.

Acknowledgement

This work was supported by NIH Grants NS18309, NS37171, and a grant from the Partnership for Pediatric Epilepsy Research (JWS), NIH Grant NS54882 (JO) and an Epilepsy Foundation Postdoctoral Fellowship (MN).

References

Al-Noori S, Swann JW. A role for sodium and chloride in kainic acid-induced beading of inhibitory interneuron dendrites. Neurosci 2000;101:337–348.

Armstrong DD. Neuropathology of Rett syndrome. J. Child. Neurol 2005;20:747–753. [PubMed: 16225830]

Barbin G, Pollard H, Gaïarsa JL, Ben-Ari Y. Involvement of $GABA_A$ receptors in the outgrowth of cultured hippocampal neurons. Neurosci. Lett 1993;152:150–154. [PubMed: 8390627]

Belichencko P, Dahlstrom A, von Essen C, Lindstrom S, Nordborg C, Sourander P. Atypical pyramidal cells in epileptic human cortex: CFLS and 3-D reconstructions. Neuroreport 1992;3:765–768. [PubMed: 1421134]

Burrone J, O'Byrne M, Murthy VN. Multiple forms of synaptic plasticity triggered by selective suppression of activity in individual neurons. Nature 2002;420:414–418. [PubMed: 12459783]

Camfield P, Camfield C. Epileptic syndromes in childhood: clinical features, outcomes, and treatment. Epilepsia 2002;43(Suppl 3):27–32. [PubMed: 12060004]

Chang YC, Huang AM, Kuo Y, Wang S, Chang YY, Huang CC. Febrile seizures impair memory and cAMP response-element binding protein activation. Annals of Neurology 2003;54:706–718. [PubMed: 14681880]

Chklovskii DB, Mel BW, Svoboda K. Cortical rewiring and information storage. Nature 2004;431:782–788. [PubMed: 15483599]

Cline HT. Dendritic arbor development and synaptogenesis. Current Opinion in Neurobiology 2001;11:118–126. [PubMed: 11179881]

Cooke BM, Woolley CS. Gonadal hormone modulation of dendrites in the mammalian CNS. J. Neurobiol 2005;64:34–46. [PubMed: 15884004]

Dailey ME, Smith SJ. The dynamics of dendritic structure in developing hippocampal slices. J. Neurosci 1996;16:2983–2994. [PubMed: 8622128]

Dalva MB, Ghosh A, Shatz CJ. Independent control of dendritic and axonal form in the developing lateral geniculate nucleus. J. Neurosci 1994;14(6):3588–3602. [PubMed: 8207474]

Desai NS, Cudmore RH, Nelson SB, Turrigiano GG. Critical periods for experience-dependent synaptic scaling in visual cortex. Nature Neuroscience 2002;5:783–789.

Dierssen M, Ramakers GJ. Dendritic pathology in mental retardation: from molecular genetics to neurobiology. Genes Brain Behav 2006;5(Suppl 2):48–60. [PubMed: 16681800]

Faherty CJ, Kerley D, Smeyne RJ. A Golgi-Cox morphological analysis of neuronal changes induced by environmental enrichment. Brain Res. Dev. Brain Res 2003;141:55–61.

Feng G, Mellor RH, Bernstein M, Keller-Peck C, Nguyen QT, Wallace M, Nerbonne JM, Lichtman JW, Sanes JR. Imaging neuronal subsets in transgenic mice expressing multiple spectral variants of GFP. Neuron 2000;28:41–51. [PubMed: 11086982]

Hardingham GE, Fukunaga Y, Bading H. Extrasynaptic NMDARs oppose synaptic NMDARs by triggering CRE shut-off and cell death pathways. Nature Neuroscience 2002;5:405–414.

Hermann BP, Seidenberg M, Bell B. The neurodevelopmental impact of childhood onset temporal lobe epilepsy on brain structure and function and the risk of progressive cognitive effects. Prog. Brain Res 2002;135:429–438. [PubMed: 12143361]

Holmes GL, Gairsa JL, Chevassus-Au-Louis N, Ben-Ari Y. Consequences of neonatal seizures in the rat: morphological and behavioral effects. Ann. Neurol 1998;44:845–857. [PubMed: 9851428]

Hua JY, Smith SJ. Neural activity and the dynamics of central nervous system development. Nature Neuroscience 2004;7:327–332.

Huang LT, Cilio MR, Silveira DC, McCabe BK, Sogawa Y, Stafstrom CE, Holmes GL. Long-term effects of neonatal seizures: a behavorial, electrophysiological, and historical study. Developmental Brain Research 1999;118:99–107. [PubMed: 10611508]

Isokawa M, Eugenio L, Mello AM. NMDA receptor-mediated excitability in dendritically deformed dentate granule cells in pilocarpine-treated rats. Neurosci. Let 1991;129:69–73. [PubMed: 1681482]

Isokawa M, Levesque MF, Babb TL, Engel J Jr. Single mossy fiber axonal systems of human dentate granule cells studied in hippocampal slices from patients with temporal lobe epilepsy. J. Neurosci 1993;13:1511–1522. [PubMed: 8463831]

Jan YN, Jan LY. The control of dendrite development. Neuron 2003;40:229–242. [PubMed: 14556706]

Jiang M, Lee CL, Smith KL, Swann JW. Spine loss and other persistent alterations of hippocampal pyramidal cell dendrites in a model of early-onset epilepsy. J Neurosci 1998;18(20):8356–8368. [PubMed: 9763479]

Jin X, Hu P, Mathers P, Agmon A. Brain-derived neurotrophic factor mediates activity-dependent dendritic growth in nonpyramid neocortical interneurons in developing organotypic cultures. J. Neurosci 2003;23(13):5662–5673. [PubMed: 12843269]

Konur S, Ghosh A. Calcium signaling and the control of dendritic development. Neuron 2005;46:401–405. [PubMed: 15882639]

Lee CL, Hannay J, Hrachovy R, Rashid S, Antalffy B, Swann JW. Recurrent seizures in infant rats produced spatial learning deficits without a substantial loss of hippocampal pyramidal cells. Neurosci 2001;107:71–84.

Lendavi B, Stern EA, Chen B, Svoboda K. Experience-dependent plasticity of dendritic spines in the developing rat barrel cortex in vivo. Nature 2000;404:876–881. [PubMed: 10786794]

Lohmann C, Myhr KL, Wong RO. Transmitter-evoked local calcium release stabilizes developing dendrites. Nature 2002;418:177–181. [PubMed: 12110889]

Luthi A, Schwyzer L, Mateos JM, Gahwiler BH, McKinney RA. NMDA receptor activation limits the number of synaptic connections during hippocampal development. Nat. Neurosci 2001;4:1102–1107. [PubMed: 11687815]

McAllister AK, Katz LC, Lo DC. Neurotrophin regulation of cortical dendritic growth requires activity. Neuron 1996;17:1057–1064. [PubMed: 8982155]

Multani P, Myers RH, Blume HW, Schomer DL, Sotrel A. Neocortical dendritic pathology in human partial epilepsy: a quantitative Golgi study. Epilepsia 1994;35:728–736. [PubMed: 7521835]

O'Brien RJ, Kamboj S, Ehlers MD, Rosen KR, Fischbach GD, Huganir RL. Activity-dependent modulation of synaptic AMPA receptor accumulation. Neuron 1998;21:1067–1078. [PubMed: 9856462]

Purpura DP, Bodick N, Suzuki K, Rapin I, Wurzelmann S. Microtubule disarray in cortical dendrites and neurobehavioral failure. 1. Golgi and electron microscopic studies. Brain Research 1982;281:287–297. [PubMed: 6185182]

Rajan I, Cline HT. Glutamate receptor activity is required for normal development of tectal cell dendrites *in vivo*. J. Neurosci 1998;18:7836–7846. [PubMed: 9742152]

Redmond L, Kashani AH, Ghosh A. Calcium regulation of dendritic growth via CaM kinase IV and CREB-mediated transcription. Neuron 2002;34:999–1010. [PubMed: 12086646]

Rhin LL, Claiborne BJ. Dendritic growth and regression in rat dentate granule cells during late postnatal development. Developmental Brain Research 1990;54:115–124. [PubMed: 2364540]

Sin WC, Haas K, Ruthazer ES, Cline HT. Dendrite growth increased by visual activity requires NMDA receptor and Rho GTPases. Nature 2002;419:475–480. [PubMed: 12368855]

Spitzer NC. Activity-dependent neuronal differentation prior to synapse formation:the functions of calcium transients. J. Physiology 2002;96:73–80.

Stoppini L, Buchs PA, Muller D. A simple method for organotypic cultures of nervous tissue. J. Neurosci. Methods 1991;37:173–182. [PubMed: 1715499]

Swann J, Al-Noori S, Jiang M, Lee CL. Spine loss and other dendritic abnormalities in epilepsy. Hippocampus 2000;10:617–625. [PubMed: 11075833]

Swann JW, Le JT, Lam TT, Owens J, Mayer AT. The Impact of Chronic Network Hyperexcitability on Developing Glutamatergic Synapses Eur. J. Neurosci. 2007ain press

Swann JW, Le JT, Lee CL. Recurrent seizures and the molecular maturation of hippocampal and neocortical glutamatergic synapses. Dev. Neurosci 2007b;29:168–178. [PubMed: 17148959]

Turrigiano GG, Leslie KR, Dasai NS, Rutherford LC, Nelson SB. Activity-dependent scaling of quantal amplitude in neocortical neurons. Nature 1998;391:845–846. [PubMed: 9495334]

Turrigiano GG, Nelson SB. Homeostatic plasticity in the developing nervous system. Nature Reviews Neuroscience 2004;5:97–107.

Vaillant AR, Zanassi P, Walsh GS, Aumont A, Alonso A, Miller FD. Signaling mechanisms underlying reversible, activity-dependent dendrite formation. Neuron 2002;34(6):985–998. [PubMed: 12086645]

Van AL, Cline HT. Rho GTPases and activity-dependent dendrite development. Curr. Opin. Neurobiol 2004;14:297–304. [PubMed: 15194109]

Ward, AA, Jr.. The epileptic neuron: chronic foci in animals and man. In: Jasper, HH.; Ward, AA.; Pope, A., editors. Basic Mechanisms of the Epilepsies. Little, Brown and Company; Boston: 1969. p. 263-298.

Watt AJ, van Rossum MCW, MacLeod KM, Nelson SB, Turrigiano GG. Activity coregulates quantal AMPA and NMDA currents at neocortical synapses. Neuron 2000;26:659–670. [PubMed: 10896161]

Wayman GA, Impey S, Marks D, Saneyoshi T, Grant WF, Derkach V, Soderling TR. Activity-dependent dendritic arborization mediated by CaM-kinase I activation and enhanced CREB-dependent transcription of Wnt-2. Neuron 2006;50:897–909. [PubMed: 16772171]

Westrum LE, White LE Jr. Ward AA Jr. Morphology of the experimental epileptic focus. J. Neurosurg 1964;21:1033–1046. [PubMed: 14279823]

Wierenga CJ, Walsh MF, Turrigiano GG. Temporal regulation of the expression locus of homeostatic plasticity. J. Neurophysiol 2006;96:2127–2133. [PubMed: 16760351]

Wong ROL, Ghosh A. Activity-dependent regulation of dendritic growth pattering. Nature Reviews Neuroscience 2002;3:803–812.

Wu GY, Cline HT. Stabilization of dendritic arbor structure in vivo by CaMKII. Science 1998;279:222–226. [PubMed: 9422694]

Wu GY, Deisseroth K, Tsien RW. Spaced stimuli stabilize MAPK pathway activation and its effects on dendritic morphology. Nat. Neurosci 2001;4:151–158. [PubMed: 11175875]

Wu GY, Zou DJ, Rajan I, Cline H. Dendritic dynamics in vivo change during neuronal maturation. J. Neurosci 1999;19:4472–4483. [PubMed: 10341248]

Yu X, Malenka RC. Beta-catenin is critical for dendritic morphogenesis. Nat. Neurosci 2003;6:1169–1177. [PubMed: 14528308]

Zha XM, Green SH, Dailey ME. Regulation of hippocampal synapse remodeling by epileptiform activity. Mol. Cell. Neurosci 2005;29:494–506. [PubMed: 15953736]

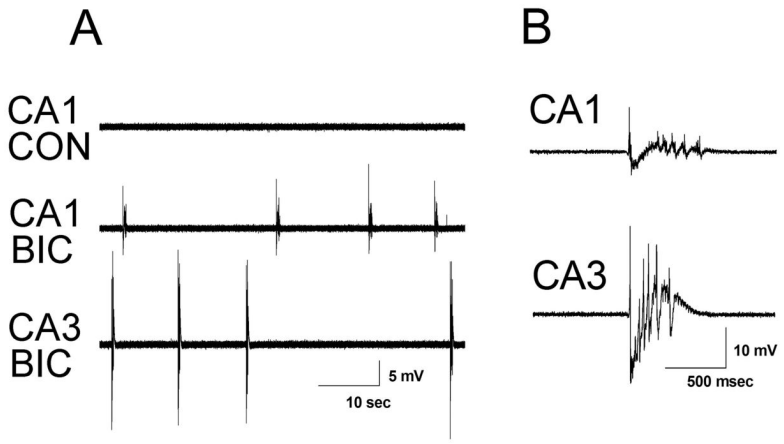

Fig. 1.

Representative traces of extracellularly recorded field activity in CA1 and CA3 from 3 DIV cultures with acute application of bicuculline. (A) Extracellular field recording from CA1 of a 3 DIV slice culture under control (CON) conditions in normal ACSF and from CA1 and CA3 of the same slice in ACSF with 50 μM bicuculline (BIC) showing synchronized epileptiform discharges. **Recordings from CA1 and CA3 were obtained sequentially**. (B) Individual extracellularly recorded bursts from CA1 and CA3, respectively, at faster time base.

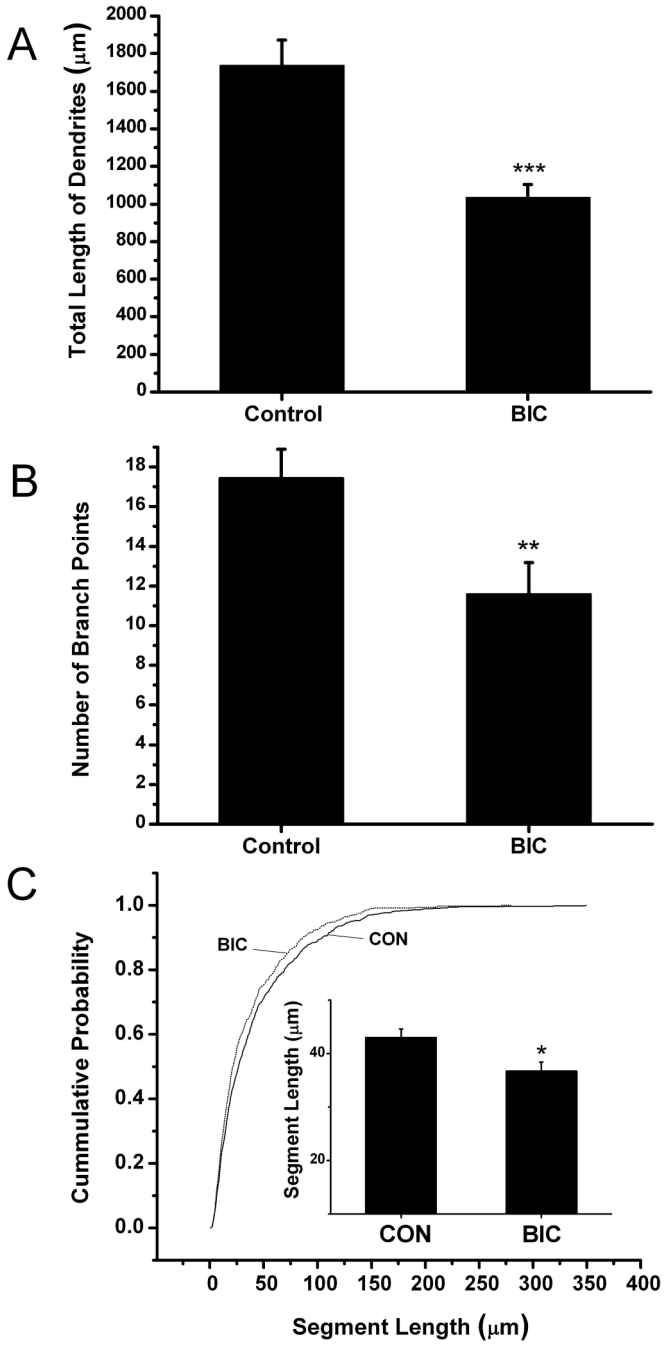

Fig. 2.

Dendritic arbor length and branching complexity are reduced following chronic disinhibition. Bar Graphs summarize results from 3 separate experiments in which the dendrites from 18 control and 17 bicuculline-treated CA1 hippocampal pyramidal cells were reconstructed. (A) Following 4 days of chronic disinhibition a decrease in basilar dendritic length was observed (***$p \leq 0.001$). (B) In addition, the number of dendritic branch points in basilar dendritic arbors was decreased significantly (**$p \leq 0.01$). (C) Cumulative distributions show that following bicuculline treatment dendritic segments are uniformly shorter than those in control slices **($p \leq 0.01$: Kolmogorov-Smirov test)**. Inset shows the average length of dendritic segments was

shorter after bicuculline treatment compared to controls (*$p \leq 0.05$). Results are presented as means ± SEM.

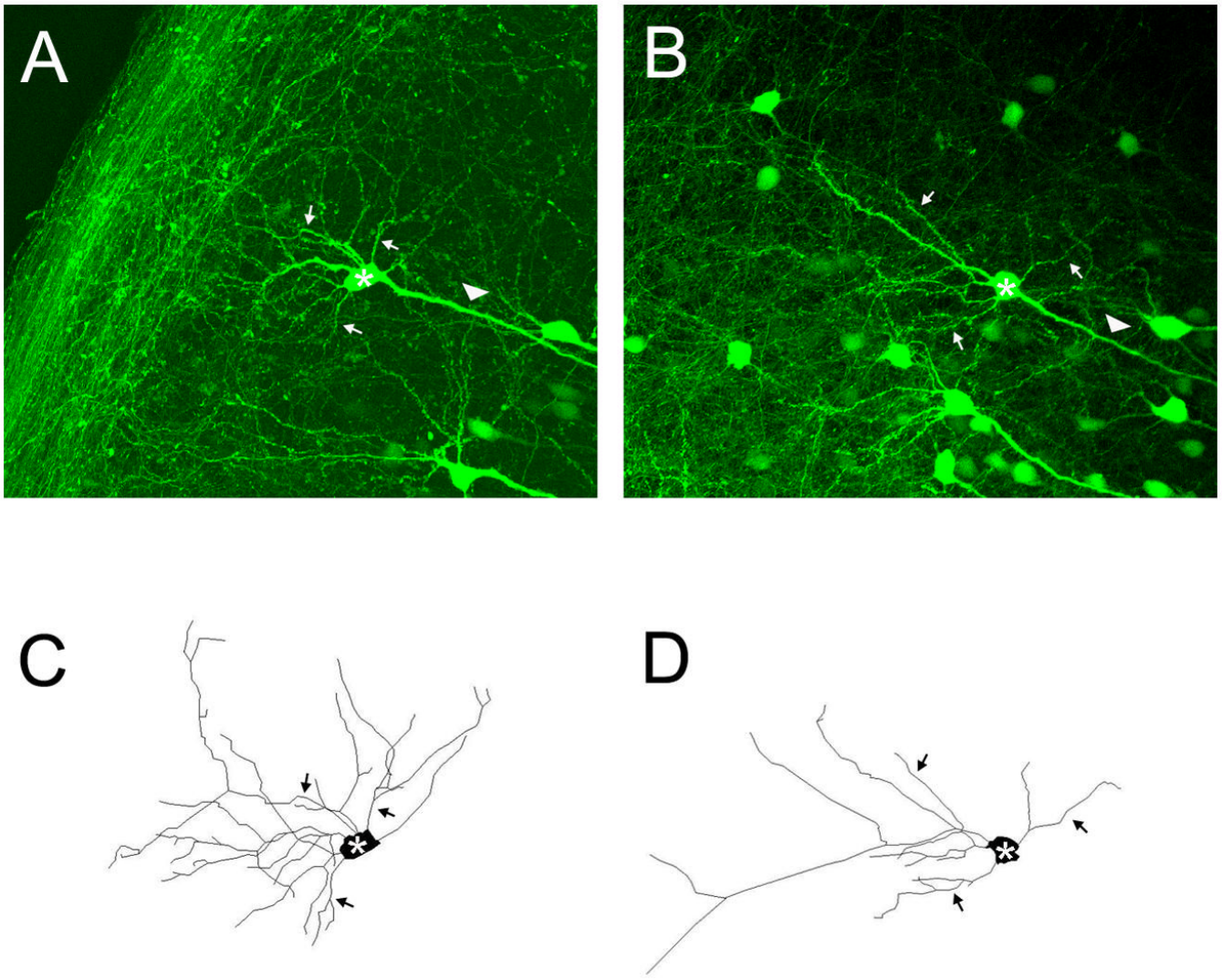

Fig. 3.

Representative images of YFP positive CA1 pyramidal neurons and reconstruction of their dendrites from control and bicuculline treated slice cultures. Maximum projection confocal images of neurons from the control (A) and bicuculline (B) treated groups. Panels C and D show Neurolucida reconstructions of the soma and basilar dendrites of these same cells and clearly illustrates that neurons treated with bicuculline have simpler dendritic arbors. For orientation, the cell bodies of the reconstructed neurons are denoted by an asterick, selected basilar dendrites by arrows and the apical dendrite by an arrow head. Apical dendrites were not reconstructed (see methods for explanation). Scale bar = 100 μm.

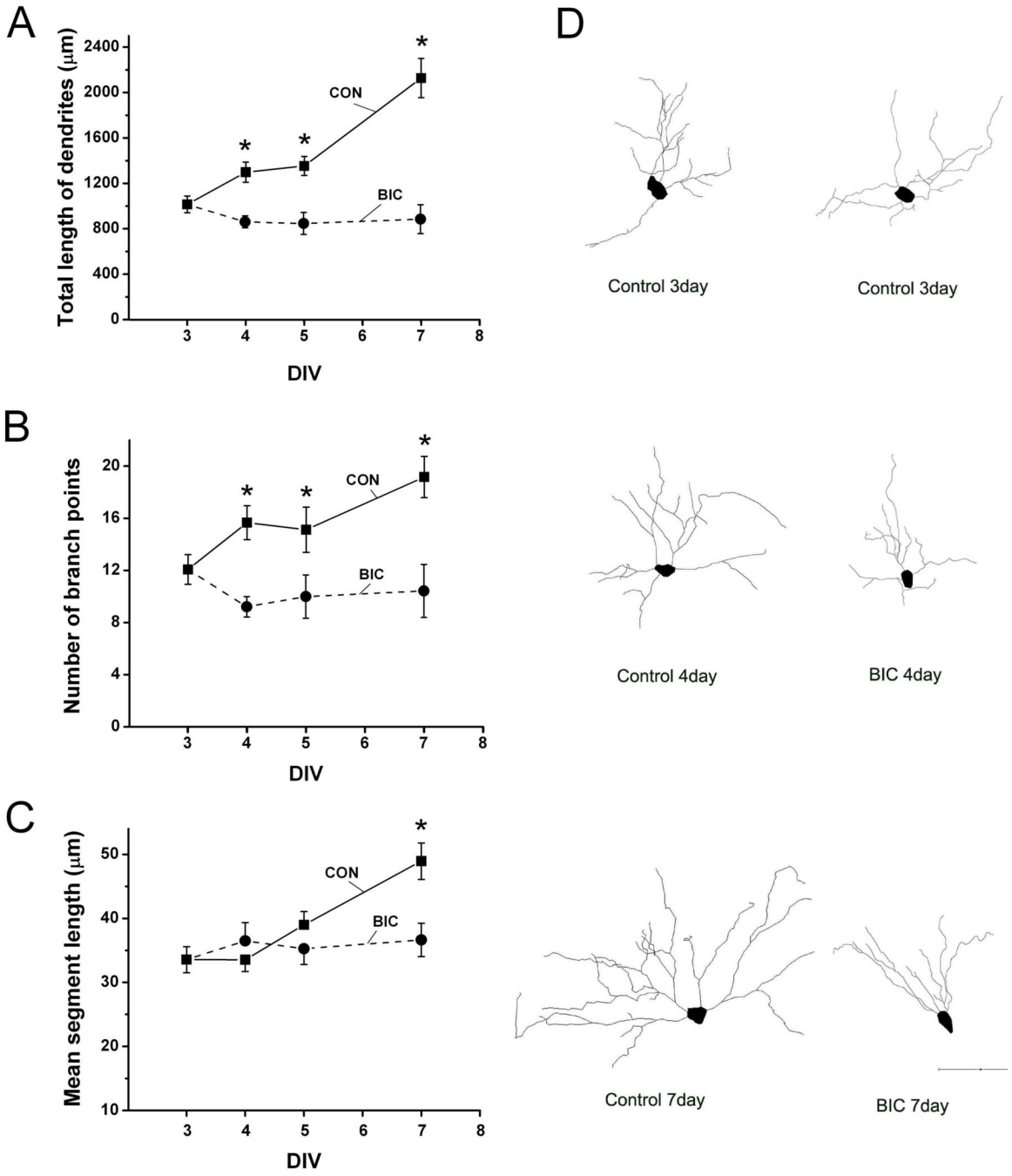

Fig. 4.

Chronic disinhibition suppresses the growth of CA1 hippocampal pyramidal cell dendrites. (A-C) Between 3 and 7 days in vitro (DIV), the dendrites of CA1 pyramidal cells in control slices gradually increased in total length, number of branch points and mean segment length. However in bicuculline treated slices, dendrites did not increase in total length (A) or average length of individual segments (C). The number of dendritic branch points appears to decrease during bicuculline treatment (B) but this effect was not statistically significant. (D) Representative Neurolucida reconstructions of dendrites of YFP positive CA1 pyramidal neurons at selected times in vitro. The soma and basilar dendrites of these cells are shown and clearly illustrate that neurons treated with bicuculline have simpler dendritic arbors compared

with controls at the same time. Number of neurons reconstructed: Control n= 6-13, Bicuculline n= 7-14. Scale bar = 100 μm. Pairwise comparison of control versus bicuculline treated dendrites on DIV 4, 5 and 7 were significantly different as indicated by * ($p \leq 0.05$).

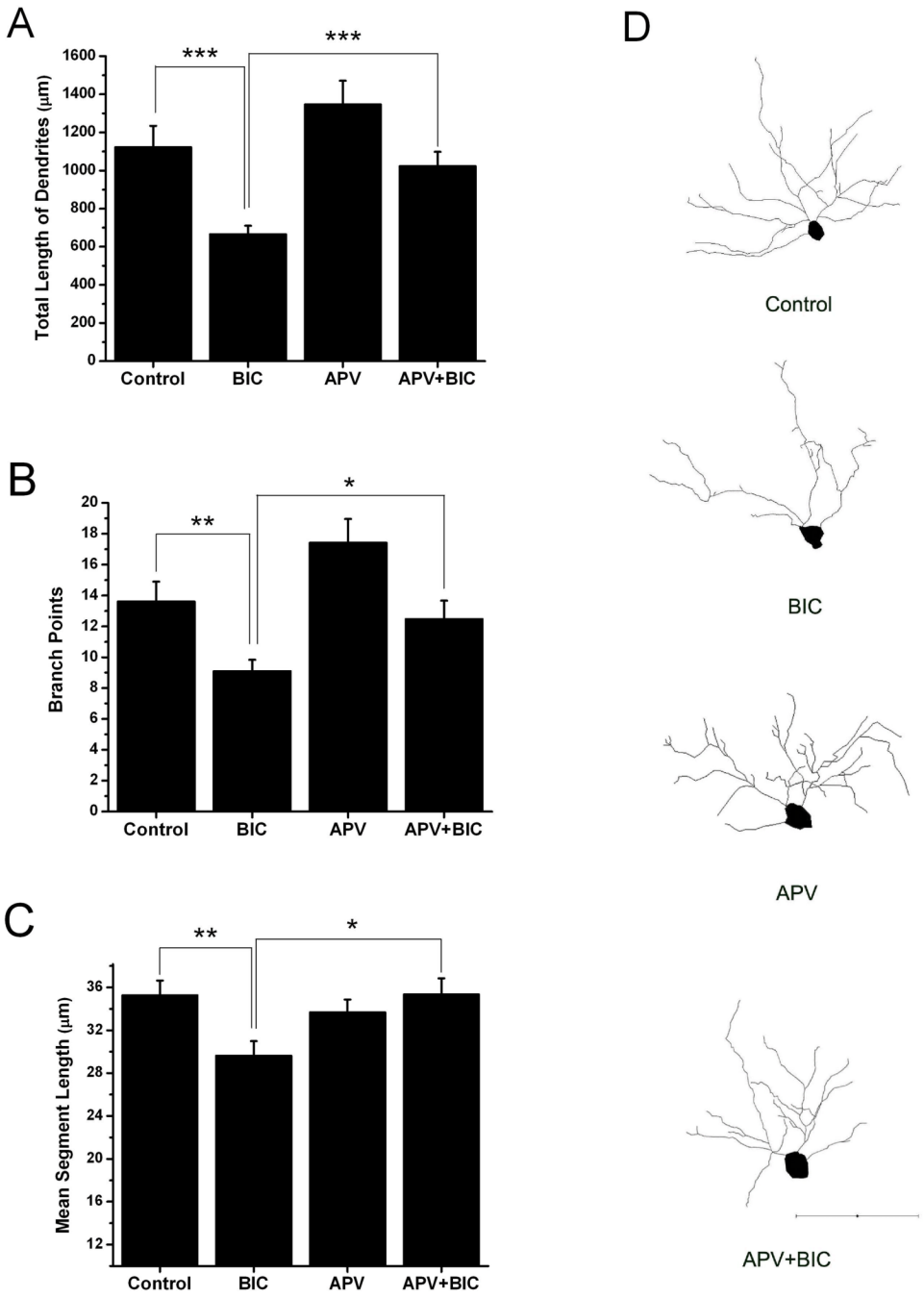

Fig. 5.

The NMDA receptor antagonist APV blocks bicuculline-induced reductions in dendritic arborization. Bar graphs show that the total length of CA1 hippocampal pyramidal cell dendrites (A), the number of branch points (B) and mean segment length (C) were all reduced by bicuculline when compared with that of control. APV alone did not significantly alter these measures of dendritic morphology but when slices were co-treated with APV and bicuculline the bicuculline-induced effects were eliminated. Only treatment with bicuculline differed statistically from controls. (D) Representative Neurolucida reconstructions of the soma and basilar dendrites of YFP positive CA1 pyramidal neurons from the four treatment groups.

Number of neurons reconstructed: Control n=18, Bicuculline n=20. APV n=19, APV+BIC n=17. Scale bar = 100 μm. (***p* ≤ 0.05, ****p* ≤ 0.01, *****p* ≤ 0.001)

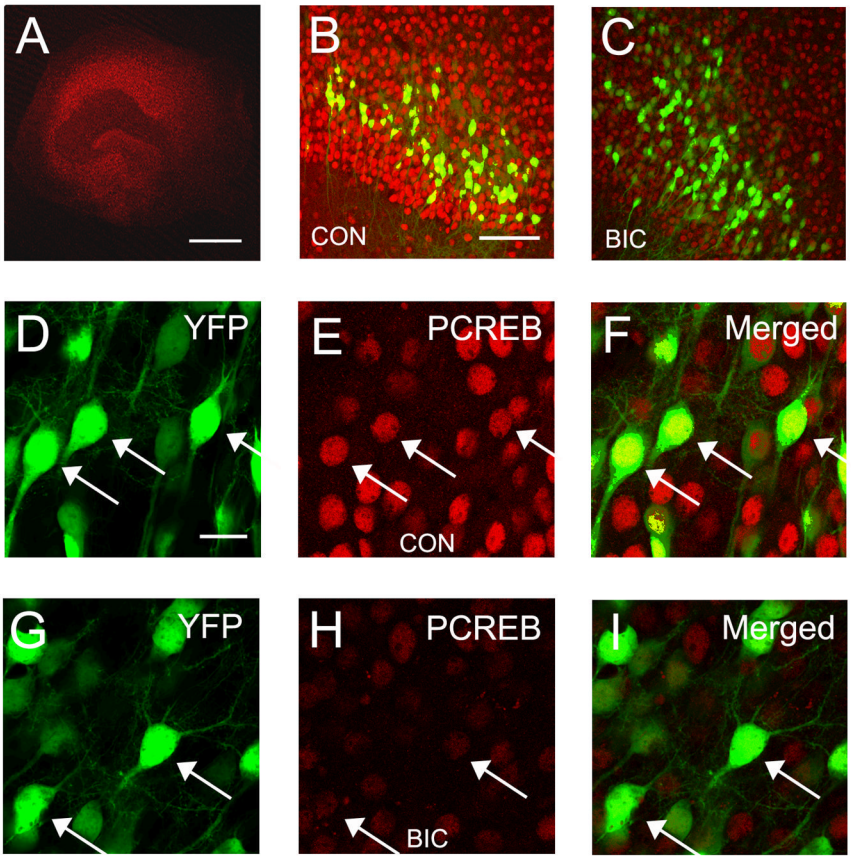

Fig. 6.

Chronic disinhibition reduces levels of phosphorylated CREB (pCREB) in CA1 hippocampal pyramidal cells. (A) Low magnification confocal image of a hippocampal slice culture showing typical pattern of immunohistochemical staining for pCREB. (B and C) Comparison of pCREB staining in hippocampal area CA1 in a control slice culture (B) and a slice treated for 4 days with bicuculline (C). Notice the dramatic reduction in expression levels of pCREB. Also shown are the subpopulation of CA1 pyramidal cells that express YFP in YFP-H mice. (D-F) The nuclear localization of pCREB is YFP-positive CA1 pyramidal cells is clearly illustrated in merged images from a control slice. (G-I) Following 4 days of bicuculline treatment pCREB immunoreactivity in CA1 pyramidal cells remains nuclear but is greatly reduced in intensity. The majority of pCREB positive -YFP negative cells are CA1 pyramidal cells that do not express YFP. Arrow heads denote sites of co-localization. Scale bars: A = 500 μm. B and C = 100 μm. D - I = 20 μm.

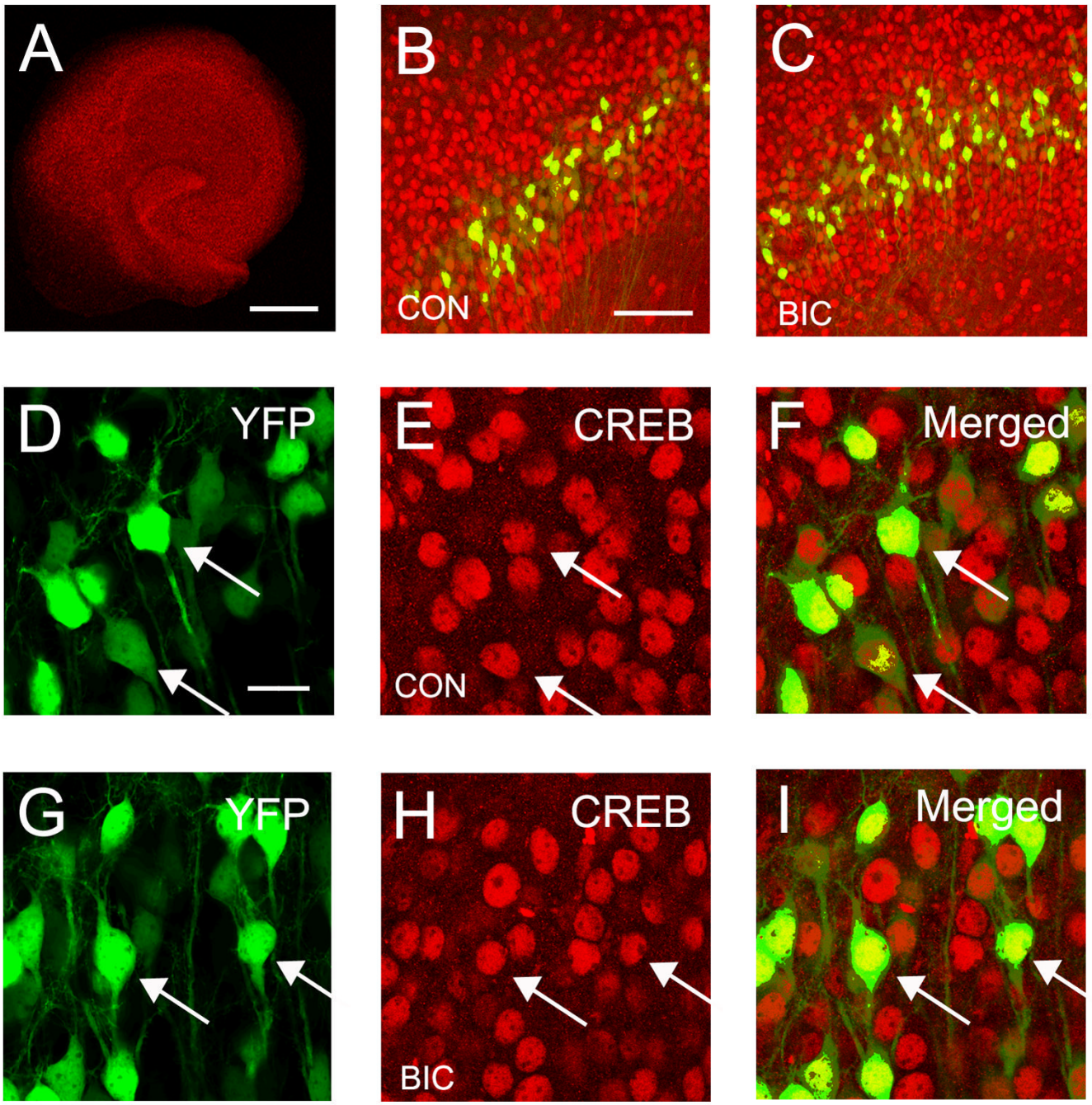

Fig. 7.

Expression of the transcription factor CREB is unaltered by chronic disinhibition. (A) Confocal image illustrating the typical pattern of CREB expression in a hippocampal slice culture. (B and C) Very similar CREB expression patterns are observed in hippocampal area CA1 in control and bicuculline treated slice cultures. YFP positive pyramidal cells are also shown in these images. (D-I) The nuclear localization of CREB in YFP positive CA1 pyramidal cells is illustrated in merged image. (G-H) The pattern and degree of CREB expression appears unaltered after 4 days of bicuculline treatment. The majority of CREB positive - YFP negative cells are CA1 pyramidal cells that do not express YFP. Arrow heads indicate co-localization of CREB and YFP signal. Calibration bars: A = 500 μm. B and C = 100 μm. D - I = 20 μm.